

GAMA: Generative Adversarial Multi-Object Scene Attacks

Abhishek Aich*, Calvin-Khang Ta*, Akash Gupta, Chengyu Song,
Srikanth V. Krishnamurthy, M. Salman Asif, Amit K. Roy-Chowdhury
University of California, Riverside, CA, USA

Abstract

The majority of methods for crafting adversarial attacks have focused on scenes with a single dominant object (e.g., images from ImageNet). On the other hand, natural scenes include multiple dominant objects that are semantically related. Thus, it is crucial to explore designing attack strategies that look beyond learning on single-object scenes or attack single-object victim classifiers. Due to their inherent property of strong transferability of perturbations to unknown models, this paper presents the first approach of using generative models for adversarial attacks on multi-object scenes. In order to represent the relationships between different objects in the input scene, we leverage upon the open-sourced pre-trained vision-language model CLIP (Contrastive Language-Image Pre-training), with the motivation to exploit the encoded semantics in the language space along with the visual space. We call this attack approach Generative Adversarial Multi-object Attacks (**GAMA**). **GAMA** demonstrates the utility of the CLIP model as an attacker’s tool to train formidable perturbation generators for multi-object scenes. Using the joint image-text features to train the generator, we show that **GAMA** can craft potent transferable perturbations in order to fool victim classifiers in various attack settings. For example, **GAMA** triggers $\sim 16\%$ more misclassification than state-of-the-art generative approaches in black-box settings where both the classifier architecture and data distribution of the attacker are different from the victim. Our code is available here: <https://abhishekaich27.github.io/gama.html>

1 Introduction

Despite attaining significant results, decision-making of deep neural network models is brittle and can be surprisingly manipulated with adversarial attacks that add highly imperceptible perturbations to the system inputs [1, 2]. This has led to dedicated research in designing diverse types of adversarial attacks that lead to highly incorrect decisions on diverse state-of-the-art classifiers [2–13]. The majority of such adversarial attacks [2, 8–18] has focused on scenes with a single dominant object (e.g., images from ImageNet [19]). However, natural scenes consist of multiple dominant objects that are semantically associated [20–25]. This calls for attack methods that are effective in such multi-object scenes.

A recent body of work in adversarial attacks [26–30] has shown the importance of exploring attack methodologies for real-world scenes (although designed for attacking object detectors). However, such methods are image-specific approaches that are known to have poor time complexity when perturbing large batches of images, as well as poor transferability to unknown models (more details in Section 2) due to their inherent property of perturbing images independently from one another.

*Equal contribution. Corresponding author: AA (aaich001@ucr.edu). AG is currently with Vimaan AI, USA.

Table 1: **Characteristic comparison.** Here, $f(\cdot)$ denotes the surrogate classifier. \mathbf{x} and \mathbf{x}_δ denote a clean and perturbed image. k denotes output from a specific pre-defined layer of $f(\cdot)$ (different for each method). Better than prior generative attacks [10–13], **GAMA** leverages multi-modal (text and image) features ρ_{txt} and ρ_{img} extracted from a pre-trained CLIP [36] model for train the perturbation generator. Its learning objective aims to pull $f_k(\mathbf{x}_\delta)$ closer to a dissimilar text embedding ρ_{txt} (w.r.t. \mathbf{x}) while pushing it away from $f_k(\mathbf{x})$ and ρ_{img} . Further, **GAMA** analyzes attack scenarios where the surrogate model is a multi-label classifier with input scenes that usually contain multiple objects.

Attack	Venue	Generator training strategy	Analyzed input scene?
GAP [10]	CVPR2018	maximize difference of $f(\mathbf{x}_\delta)$ and $f(\mathbf{x})$	single object
CDA [11]	NeurIPS2019	maximize difference of $f(\mathbf{x}_\delta) - f(\mathbf{x})$ and $f(\mathbf{x})$	single object
TAP [12]	NeurIPS2021	maximize difference of $f_k(\mathbf{x}_\delta)$ and $f_k(\mathbf{x})$	single object
BIA [13]	ICLR2022	maximize difference of $f_k(\mathbf{x}_\delta)$ and $f_k(\mathbf{x})$	single object
GAMA	Ours	contrast $f_k(\mathbf{x}_\delta)$ w.r.t. ρ_{txt} , ρ_{img} and $f_k(\mathbf{x})$	single/ multiple objects

2 Related works

Adversarial attacks on classifiers. Several state-of-the-art adversarial attacks [2, 6, 8–17, 52–60] have been designed to disturb the predictions of classifiers. Broadly these approaches can be categorized into two strategies: instance (or image) specific attacks and generative model-based attacks. Instance specific attacks [2, 6, 8, 9, 14–17, 52–60] create perturbations for every image exclusively. Specifically, these perturbations are computed by querying the victim model for multiple iterations in order to eventually alter the image imperceptibly (e.g. texture level changes to image [60]) to cause its misclassification. Due to this “specific to image” strategy, their time-complexity to alter the decision of a large set of images has been shown to be extremely poor [11, 13, 31]. Furthermore, learning perturbations based on single-image generally restrict their success of misclassification only on the known models [11, 13].

To alleviate these drawbacks, a new category of attack strategies has been explored in [10–13, 61] where a generative model is adversarially trained against a surrogate victim model (in other words, treated as a *discriminator*) to craft perturbations on whole data distribution. This attack strategy particularly allows one to perturb multiple images simultaneously once the generative model is optimized, as well as enhances the transferability of perturbations to unseen black-box models [10, 11]. For example, Generative Adversarial Perturbations or GAP [10] and Cross-Domain Attack or CDA [11] presented a distribution-driven attack that trains a generative model for creating adversarial examples by utilizing the cross-entropy loss and relativistic cross-entropy loss [62] objective, respectively. Different from these, Transferable Adversarial Perturbations or TAP [12] and Beyond ImageNet Attack or BIA [13] presented an attack methodology to further enhance transferability of perturbations using feature separation loss functions (e.g. mean square error loss) at mid-level layers of the surrogate model. Most of these methods focused on creating transferable perturbations assuming that the surrogate model is trained in the same domain as the target victim model [13]. Further, a mid-level layer is manually selected for each architecture and is also sensitive to the dataset (shown later in Section 4). Similarly, [61] proposes to change image attributes to create semantic manipulations using their disentangled representations via generative models. Most of these generative attacks employed classifiers that operate under the regime that input images include single dominant objects. Some recent attacks [26–30] have focused on analyzing complex images which contain multiple objects, however, they are instance-driven attacks that introduce aforesaid drawbacks of transferability and time complexity. In contrast to these aforementioned works, **GAMA** is a generative model-based attack designed to craft imperceptible adversarial perturbations that can strongly disrupt both multi-label and single-label classifiers. Moreover, **GAMA** uses a novel perturbation generation strategy that employs a pre-trained CLIP model [36] based framework to craft highly effective and transferable perturbations by leveraging multi-modal (image and text) embeddings. We summarize the differences between prior generative attacks and **GAMA** in Table 1.

Applications of Vision-and-Language (VL) representations. Due to their robust zero-shot performance, joint vision-and-language pre-trained models [35–39] have allowed new language-driven solutions for various downstream tasks [40–51, 63]. The differentiating attribute of using VL models [36], when compared to existing conventional image-based pre-trained models [33], is that they provide high-quality aligned visual and textual representations learnt from large-scale image-text

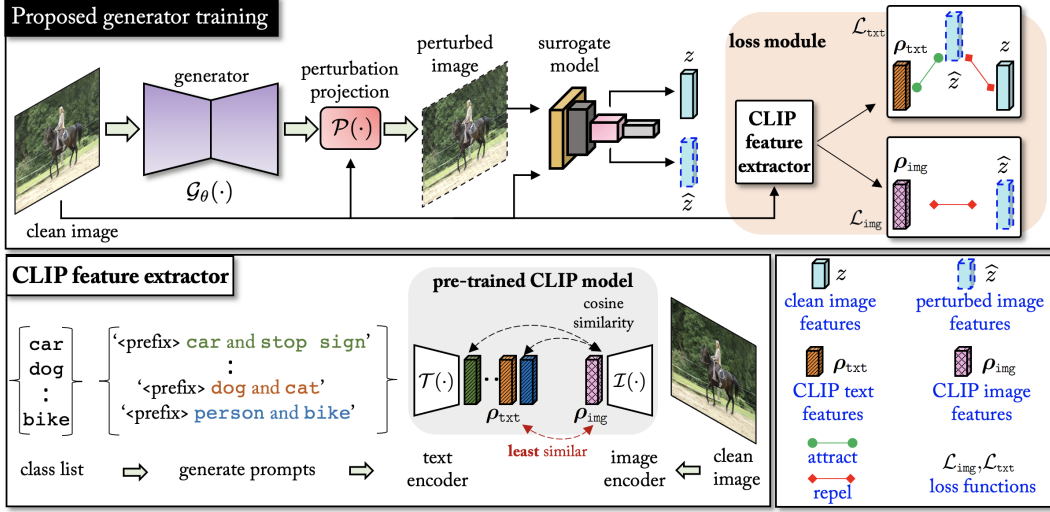


Figure 2: **Overview of GAMA.** The perturbation generator $\mathcal{G}_\theta(\cdot)$ crafts a perturbed image (ℓ_∞ -budget constrained by projection operator $\mathcal{P}(\cdot)$) from the clean image as input. Next, embeddings z from clean image and \hat{z} from perturbed image are extracted from the surrogate model. A pre-trained CLIP model extracts the image embedding ρ_{img} from the clean image and the text embedding ρ_{txt} that is *least* similar to ρ_{img} (see details in Section 3.1). Finally, the loss functions \mathcal{L}_{img} and \mathcal{L}_{txt} utilize these embeddings to optimize the generator weights θ . Loss solely based on a surrogate model not shown here for simplicity. We use a *prefix*='a photo depicts' in all the text prompts following [67].

pairs. In this work, we leverage one such powerful VL framework named CLIP [36] to an adversary's advantage and show its utility in preparing a perturbation generator for formidable attacks across multiple distributions. Employing freely available pre-trained models for tasks other than what they were trained for has been common practice (e.g. VGG [64] models in [65, 66], CLIP for domain adaptation of generators in [46]). To the best of our knowledge, the proposed attack is the first to introduce such VL model usage to subvert classifier decisions.

3 Proposed Attack Methodology: GAMA

Problem Statement. Our goal is to train a generative model $\mathcal{G}_\theta(\cdot)$ (weights θ) from a training distribution of images with multiple-objects. Once θ is optimized, $\mathcal{G}_\theta(\cdot)$ can create perturbations on diverse types (multi-object or otherwise) of input images that can lead to misclassification on an unknown victim classifier. Suppose we have access to a *source* dataset \mathcal{D} consisting of N training samples from C number of classes, with each sample/image possibly consisting of multiple object labels, i.e., multi-label images. Each i^{th} sample in \mathcal{D} is represented as $\mathbf{x}^{(i)} \in \mathbb{R}^{H \times W \times T}$ (with height H , width W , and channels T) containing labels $\mathbf{y}^{(i)} = [y_1^{(i)}, \dots, y_C^{(i)}] \in \mathcal{Y} \subseteq \{0, 1\}^C$. More specifically, if sample $\mathbf{x}^{(i)}$ is associated with class c , $y_c^{(i)} = 1$ indicates the existence of an object from class c in $\mathbf{x}^{(i)}$. Further, we have access to a surrogate multi-label classifier trained on \mathcal{D} denoted as $\mathbf{f}(\cdot)$ which is employed to optimize the perturbation generator $\mathcal{G}_\theta(\cdot)$'s weight θ . For ease of exposition, we drop the superscript i in further discussion.

3.1 Adversary Equipped with Pre-Trained CLIP

We aim to train a generator $\mathcal{G}_\theta(\cdot)$ that learns to create perturbations from its observations by fooling a surrogate classifier $\mathbf{f}(\cdot)$ during its training phase. Now, as $\mathcal{G}_\theta(\cdot)$ learns to create perturbations δ in accordance to $\mathbf{f}(\cdot)$, it is bounded by the features extracted from $\mathbf{f}(\cdot)$ in order to contrast \mathbf{x} and \mathbf{x}_δ (e.g. final-layer logits in [10, 11] or mid-level features [12, 13]). In this work, we explore a case where we have access to a pre-trained vision-and-language model like CLIP that can be utilized as a loss network to train $\mathcal{G}_\theta(\cdot)$. Our motivation for using CLIP is to exploit its joint text and image matching property and compute two embeddings: clean image embedding extracted from the image encoder and a *dissimilar* text embedding extracted from the text encoder. Specifically, we aim to encode

the contextual relationships between multiple objects in the natural scene via language derivatives. We next describe **GAMA**'s method and present a novel strategy to use CLIP's model to train $\mathcal{G}_\theta(\cdot)$. Note that we assume each image contains two co-occurring classes for creating text prompts, mainly restricted due to computation of co-occurrence matrices of dimension $C \times C$ available for multi-label datasets. As we will see later, co-occurrence matrices allow us to discard pairs of classes that would not occur in real-world scenarios.

GAMA Overview. Before training $\mathcal{G}_\theta(\cdot)$, we first compute a text embedding matrix $\mathbf{A}_{\text{txt}} = [\rho_1, \rho_2, \dots, \rho_N] \in \mathbb{R}^{N \times K}$ with $\rho_n \in \mathbb{R}^K$ (explained in detail later) using the CLIP text encoder $\mathcal{T}(\cdot)$. Here, K is the embedding size of output from $\mathcal{T}(\cdot)$. During training $\mathcal{G}_\theta(\cdot)$, we start by feeding the clean image x to the CLIP image encoder $\mathcal{I}(\cdot)$ and computing an image embedding $\rho_{\text{img}} = \mathcal{I}(x) \in \mathbb{R}^K$. Next, a particular vector $\rho_{\text{txt}} \in \mathbb{R}^K$ from \mathbf{A}_{txt} is retrieved that is least similar to ρ_{img} . Then, we feed x to $\mathcal{G}_\theta(\cdot)$ and create x_δ while ensuring it to be under given perturbation ℓ_∞ budget ϵ using the perturbation projection operator $\mathcal{P}(\cdot)$. These clean and perturbed images are then fed to the surrogate classifier $f(\cdot)$ to extract K -dimensional embeddings at specific k th layer, denoted by $f_k(x)$ and $f_k(x_\delta)$ respectively. Finally, the aforementioned quadruplet embeddings $(\rho_{\text{txt}}, \rho_{\text{img}}, f_k(x), f_k(x_\delta))$ are used to compute a contrastive learning based CLIP text embedding-guided loss $\mathcal{L}_{\text{txt}}(\rho_{\text{txt}}, f_k(x), f_k(x_\delta))$ and a regression learning based CLIP image embedding-guided loss $\mathcal{L}_{\text{img}}(\rho_{\text{img}}, f_k(x_\delta))$ to compute the final objective \mathcal{L} . We also include a loss function that further maximizes the difference between $f_k(x)$ and $f_k(x_\delta)$ solely from the surrogate classifier's perspective. This loss \mathcal{L} is minimized to update the weights of the generator θ . The whole **GAMA** paradigm is illustrated in Figure 2 and summarized in Algorithm 1. The details of loss objectives \mathcal{L}_{img} and \mathcal{L}_{txt} (with text embedding matrix \mathbf{A}_{txt}) are discussed next.

CLIP text embedding-guided loss (\mathcal{L}_{txt}). Let $z = f_k(x)$ and $\hat{z} = f_k(x_\delta)$. The CLIP framework inherently learns the text and vision embedding association via a contrastive learning regime [36, 68], constraining the feature embeddings of the input image and its counterpart language description to be as similar as possible. Different from CLIP's image embedding ρ_{img} , CLIP's text embedding ρ_{txt} allows us to look beyond the pixel-based features. More specifically, CLIP's vision-and-language aligning ability allows us to utilize *text* features to craft transferable image perturbations. Hence, we can optimize $\mathcal{G}_\theta(\cdot)$ to create perturbed images x_δ that do not follow the same text embedding alignment as their clean image counterpart x . In order to cause this text misalignment, we create a triplet of embeddings where the anchor \hat{z} is pushed away from z while pulling it closer to a text embedding ρ_{txt} that is least associated or similar to a clean image x . To compute this triplet, the following two steps are performed.

- **Before training, compute \mathbf{A}_{txt} .** The goal is create a dictionary or matrix of text embeddings which can be utilized to retrieve ρ_{txt} during optimization of $\mathcal{G}_\theta(\cdot)$. Firstly, we generate language derivatives or *text prompts* using classes of source distribution. This means we only need to know all the available C classes in \mathcal{D} but not their specific association with x . Secondly, with assumption that each clean image x is associated with two classes, we can generate C^2 text prompts and create a matrix \mathbf{A}_{txt} of size $C^2 \times K$. For example, if classes 'cat', 'dog', 'person' and 'boat' exist in \mathcal{D} , then one can create text prompts such as "a photo depicts cat and dog" or "a photo depicts person and boat" (see Figure 1 for 10 random examples extracted from CLIP's 'ViT-B/16' model using Pascal-VOC's classes). Here, the part of the text prompt underlined is a recommended 'prefix' common to all text prompts as suggested in [67]. However, such \mathbf{A}_{txt} can contain embeddings from prompts that are generated from classes that do not exist in real life. To circumvent this, we utilize an object co-occurrence matrix $\mathcal{O} \in \mathbb{R}^{C \times C}$ (a binary matrix) to estimate the co-occurrence relationships between classes. Computed from the training data set containing C classes, \mathcal{O} is first initialized with a matrix containing only zeros. Then, an element \mathcal{O}_{ij} (i th row and j th column of \mathcal{O}) is set to 1 if objects from classes y_i and y_j appear together at least in one image. Computing such co-occurrence information is a common practice in multi-object downstream problems [26, 27, 69–72]. We use \mathcal{O} provided by [69]. Using such a co-occurrence matrix, we only create text prompts from a pair of classes that occur together according to \mathcal{O} . This leads to a text embedding matrix of size \mathbf{A}_{txt} of size $\|\mathcal{O}\|_0 \times K$ where $\|\mathcal{O}\|_0$ denotes total non-zero elements.
- **During training, compute ρ_{txt} .** CLIP's training objective allows it to push the embeddings of associated image-text pairs closer compared to non-matched pairs. We leverage this property to compute the least similar text embedding ρ_{txt} w.r.t. image embedding ρ_{img} . During each training

epoch, we randomly sample B candidates $[\rho_1, \rho_2, \dots, \rho_B]$ from \mathbf{A}_{txt} and estimate ρ_{txt} as follows:

$$\rho_{\text{txt}} = \min[\text{cs}(\rho_{\text{img}}, \rho_1), \text{cs}(\rho_{\text{img}}, \rho_2), \dots, \text{cs}(\rho_{\text{img}}, \rho_B)] \quad (1)$$

Here, $\text{cs}(\cdot)$ denotes cosine similarity. Next, we force \hat{z} to align with ρ_{txt} while misaligning with z . This is implemented as contrastive learning [73, 74] objective as follows.

$$\mathcal{L}_{\text{txt}} = \min_{\theta} \frac{1}{K} \left(\|\hat{z} - \rho_{\text{txt}}\|_2^2 + [\alpha - \|\hat{z} - z\|_2]_+ \right) \quad (2)$$

where $\alpha > 0$ is the desired margin between clean and perturbed image embedding, and $[v]_+ = \max(0, v)$. \mathcal{L}_{txt} pulls away embeddings of x and x_δ by making them keep a margin α while pushing dissimilar embeddings \hat{z} and ρ_{txt} closer than the given margin.

CLIP image embedding-guided loss (\mathcal{L}_{img}). Due to CLIP’s learning on ~ 400 million internet retrieved images from diverse categories and its consequential strong zero-shot image recognition performance over different distributions [36, 41], we argue that its image encoder $\mathcal{I}(\cdot)$ outputs an embedding that has captured attributes of input image with distinct generalized visual features. **GAMA** leverages this to our advantage, and maximizes the difference between \hat{z} and CLIP’s image encoder’s embedding for clean image ρ_{img} . The aim of such an objective is to increase the transferability strength of $\mathcal{G}_\theta(\cdot)$ perturbations using the generalized features computed from $\mathcal{I}(\cdot)$. This is envisioned using a regression learning based loss described as follows:

$$\mathcal{L}_{\text{img}} = \min_{\theta} - \left(\frac{1}{K} \|\rho_{\text{img}} - \hat{z}\|_2^2 \right) \quad (3)$$

Final Learning Objective (\mathcal{L}). Loss functions \mathcal{L}_{img} and \mathcal{L}_{txt} are finally added to a surrogate model loss \mathcal{L}_{sur} that minimizes the cosine similarity of z and \hat{z} [13]. Choice of layer k is dependent on feature outputs of the CLIP model employed. All embeddings are normalized before computing the loss functions.

$$\mathcal{L} = \min_{\theta} (\mathcal{L}_{\text{sur}} + \mathcal{L}_{\text{img}} + \mathcal{L}_{\text{txt}}) \quad (4)$$

Overall, \mathcal{L}_{sur} maximizes the difference between x and x_δ from surrogate $f(\cdot)$ ’s perspective, while \mathcal{L}_{img} and \mathcal{L}_{txt} enhance its transferability using CLIP’s perspective.

Attack evaluation. We assume that the attacker has no knowledge of victim classifier $g(\cdot)$ and its data distribution \mathcal{D}_t . Further, there is a perturbation budget of ϵ defined by an ℓ_∞ norm. To launch an attack, we input a clean image x_t from target dataset \mathcal{D}_t to optimized $\mathcal{G}_\theta(\cdot)$ and craft imperceptible perturbations δ_t in order to alter the decision space of the target victim classifier $g(\cdot)$ (pre-trained on \mathcal{D}_t). Mathematically, this can be represented as $y_t \neq \hat{y}_t$ where, $y_t = g(x_t)$ and $\hat{y}_t = g(x_t + \delta_t)$ with $\|\delta_t\|_\infty \leq \epsilon$. We can cause following attack scenarios after training $\mathcal{G}_\theta(\cdot)$ against $f(\cdot)$ on \mathcal{D} :

- *Scenario 1:* an attack termed *white-box* if $f(\cdot) = g(\cdot)$ and $\mathcal{D} = \mathcal{D}_t$
- *Scenario 2:* an attack termed *black-box* if either $f(\cdot) \neq g(\cdot)$ or $\mathcal{D} \neq \mathcal{D}_t$

A real-world attack is generally modeled by *Scenario 2* as an adversary would not have the knowledge of victim model $g(\cdot)$ ’s architecture, its training data distribution \mathcal{D}_t and the task it performs *e.g.* single-label classification, multi-label classification, or object detection, *etc.* The perturbations that make an attack successful in *Scenario 2* should be highly transferable.

4 Experiments

In this section, we analyze the strength of **GAMA** under diverse practical attack settings. We also perform an ablation analysis of **GAMA**, test the attack robustness against various defenses ([76, 77], median blurring, context-consistency check), as well performance of attacks on different architecture designs. *Note that* we provide more black-box attack results in the supplementary material.

Baselines. As there are no prior works for generative attacks that learn on multi-object scenes using multi-label classifiers, we define our baselines by adapting existing state-of-the-art generative attacks summarized in Table 1. Specifically, the cross-entropy loss in GAP [10] and CDA [11] is replaced with binary cross-entropy loss to handle the prediction of multiple labels during training.

Training Details. We use the multi-label datasets PASCAL-VOC [78] and MS-COCO [79] to train

Algorithm 1: GAMA pseudo-code

Input : distribution \mathcal{D} , batch size B , perturbation ℓ_∞ bound ϵ
Input : surrogate classifier $\mathbf{f}(\cdot)$, CLIP-encoders for text $\mathcal{T}(\cdot)$ and image $\mathcal{I}(\cdot)$
Output : optimized perturbation generator $\mathcal{G}_\theta(\cdot)$'s weights θ

- 1 Randomly initialize θ . Load (as well as freeze) $\mathbf{f}(\cdot)$, $\mathcal{T}(\cdot)$ and $\mathcal{I}(\cdot)$ with respective pre-trained weights
- 2 Create text embeddings matrix \mathbf{A}_{txt} from $\mathcal{T}(\cdot)$ as described in Section 3.1
- 3 **repeat**
- 4 Input \mathbf{x} to $\mathcal{I}(\cdot)$ and get ρ_{img}
- 5 Randomly sample B vectors from \mathbf{A}_{txt} and get least similar text embedding ρ_{txt} w.r.t. ρ_{img}
- 6 Input clean image \mathbf{x} (from \mathcal{D}) to $\mathbf{f}(\cdot)$ and compute mid-level embedding $\mathbf{f}_k(\mathbf{x})$
- 7 Input \mathbf{x} to $\mathcal{G}_\theta(\cdot)$ and project it within bound ϵ using $\mathcal{P}(\cdot)$ to obtain \mathbf{x}_δ
- 8 Input \mathbf{x}_δ to $\mathbf{f}(\cdot)$ and compute mid-level embedding $\mathbf{f}_k(\mathbf{x}_\delta)$
- 9 Compute loss \mathcal{L} by Equation (4) and minimize it to update θ using Adam [75]
- 10 **until** convergence

generators for the baselines and our method. Unless otherwise stated, perturbation budget is set to $\ell_\infty \leq 10$ for all experiments. We chose the following surrogate models $\mathbf{f}(\cdot)$ (Pascal-VOC or MS-COCO pre-trained multi-label classifiers): ResNet152 (Res152) [80], DenseNet169 (Den169) [81], and VGG19 [64]. For the CLIP model, we use the ‘ViT-B/16’ framework [36]. See supplementary material for more training details.

Inference Metrics. We measure attack performances on multi-label classifiers using hamming score (%) defined in [82, 83]. For evaluations on single-label classifiers and object detectors, we use top-1 accuracy (%) and bbox_mAP_50 $\in [0, 1]$ metric, respectively. A lower score indicates better attack. Best results are in **bold**. For reference, accuracy on clean images is provided as ‘No Attack’.

4.1 Results and Analysis

All trained perturbation generators (trained only on multi-label datasets) are extensively evaluated under following victim model settings.

- *White-box and black-box (multi-label classification, different model than $\mathbf{f}(\cdot)$):* We evaluate the attacks in white-box and black-box settings on six victim multi-label classifiers (VGG16, VGG19, ResNet50 (Res50), Res152, Den169, and DenseNet121 (Den121)) in Table 2 and Table 3 (white-box attacks are marked with cell color). We outperform all baselines in the majority of cases, with an average absolute difference (w.r.t. closest method) of ~ 13 percentage points (pp) for Pascal-VOC and ~ 4.46 pp for MS-COCO.

- *Black-box (single-label classification):* We evaluate the attacks in a black-box setting with various single-label classifiers for CIFAR10/100 [84] (coarse-grained tasks [13]), CUB-200-2011 (CUB) [32], Stanford Cars (Car) [85], and FGVC Aircrafts (Air) [86] (fine-grained tasks [13]) in Table 6, and ImageNet [87] (50K validation set) in Table 4 and Table 5. Following [13], the victim models of coarse-grained tasks are taken from [88], fine-grained task models (Res50, SENet154 (SeNet), and SE-ResNet101 (se-Res101) [89]) from [90], and six ImageNet models from [33]. Here, we beat our closest baseline in all cases by ~ 13.33 pp for Pascal-VOC and ~ 5.83 pp for MS-COCO on six ImageNet models. Note that the ImageNet results also demonstrate the drop in performance of TAP [12] and BIA [13] attacks that show close to 0% top-1 accuracy when $\mathcal{G}_\theta(\cdot)$ is trained on ImageNet on the attacker side [12, 13]. We hypothesize that such a drop in performance is due to sensitivity to the dataset of the manually selected mid-level layer of $\mathbf{f}(\cdot)$ used by the attacker. We observe a similar trend when attacking non-ImageNet distributions as suggested by BIA [13] in coarse and fine-grained tasks in Table 6. In this case, **GAMA** beats the prior attacks by average ~ 13.33 pp when $\mathcal{G}_\theta(\cdot)$ is trained with Pascal-VOC.

- *Black-box (Object detection):* We also evaluate a difficult black-box attack with state-of-the-art MS-COCO object detectors (Faster RCNN with Res50 backbone (FRCN) [91], RetinaNet with Res50 backbone (RNet) [92], DETection TRansformer (DETR) [93], and Deformable DETR (D²ETR) [94]) in Table 7, available from [95]. It can be observed that **GAMA** outperforms its competitors when $\mathcal{G}_\theta(\cdot)$ is trained with Pascal-VOC.

Table 2: Pascal-VOC \rightarrow Pascal-VOC

$f(\cdot)$	Method	VGG16	VGG19	Res50	Res152	Den169	Den121	Average
VGG19	No Attack	82.51	83.18	80.52	83.12	83.74	83.07	82.69
	GAP [10]	19.64	16.60	72.95	76.24	68.79	66.50	53.45
	CDA [11]	26.16	20.52	61.40	65.67	70.33	62.67	51.12
	TAP [12]	24.77	19.26	66.95	66.95	68.65	64.51	51.84
	BIA [13]	12.53	14.00	64.24	69.07	69.44	64.71	48.99
	GAMA	6.11	5.89	41.17	45.57	53.11	44.58	32.73
Res152	GAP [10]	56.93	56.20	65.58	72.26	75.22	69.54	65.95
	CDA [11]	41.07	47.60	53.84	47.22	67.50	59.65	52.81
	TAP [12]	52.92	58.24	56.52	53.61	71.55	64.56	59.56
	BIA [13]	45.34	49.74	51.98	50.27	67.75	61.05	54.35
	GAMA	33.42	39.42	32.39	20.46	49.76	49.54	37.49
	GAP [10]	62.09	59.55	68.60	72.81	76.09	72.70	68.64
Den169	CDA [11]	52.28	53.75	59.65	67.23	69.60	67.37	61.64
	TAP [12]	58.48	58.55	58.14	63.42	52.66	62.57	58.97
	BIA [13]	48.52	53.77	56.15	63.33	54.01	58.85	55.77
	GAMA	44.25	52.89	48.83	53.25	45.00	50.96	49.19

Table 3: MS-COCO \rightarrow MS-COCO

$f(\cdot)$	Method	VGG16	VGG19	Res50	Res152	Den169	Den121	Average
VGG19	No Attack	65.80	66.48	65.64	67.95	67.59	66.39	66.64
	GAP [10]	8.31	10.61	39.49	48.00	41.00	38.12	30.92
	CDA [11]	6.57	8.57	37.38	43.56	38.41	35.59	28.34
	TAP [12]	3.45	6.14	25.77	29.56	20.05	21.15	17.68
	BIA [13]	2.47	4.01	30.76	37.34	26.40	27.95	21.48
	GAMA	3.59	3.75	27.13	30.43	24.60	21.77	18.54
Res152	GAP [10]	42.59	45.41	51.22	53.75	54.18	52.54	49.94
	CDA [11]	30.16	37.79	42.83	45.13	49.24	44.93	41.68
	TAP [12]	24.34	25.94	29.40	24.13	35.58	33.06	28.74
	BIA [13]	22.73	22.76	28.64	22.16	36.06	32.41	27.46
	GAMA	24.52	27.73	30.62	23.04	31.30	27.31	27.42
	GAP [10]	29.85	32.77	38.15	40.84	24.98	33.99	33.43
Den169	CDA [11]	39.39	41.19	46.34	50.82	43.42	44.63	44.29
	TAP [12]	23.01	27.73	32.75	40.22	15.73	20.90	26.72
	BIA [13]	27.01	29.59	34.65	43.42	13.57	24.69	28.82
	GAMA	10.40	13.47	19.30	23.46	8.65	10.29	14.26

Table 4: Pascal-VOC \rightarrow ImageNet

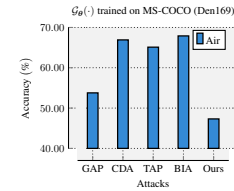
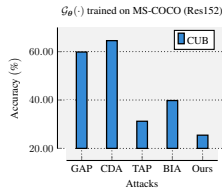
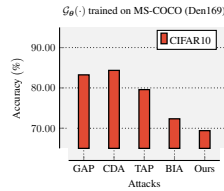
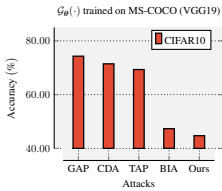
$f(\cdot)$	Method	VGG16	VGG19	Res50	Res152	Den121	Den169	Average
VGG19	No Attack	70.15	70.94	74.60	77.34	74.22	75.74	73.83
	GAP [10]	24.44	21.64	63.65	67.84	63.09	65.47	51.02
	CDA [11]	13.83	11.99	47.32	53.92	46.81	52.24	37.68
	TAP [12]	06.70	07.28	50.94	57.36	47.68	53.43	37.23
	BIA [13]	04.20	04.73	48.63	57.65	45.94	53.37	35.75
	GAMA	03.07	03.41	22.32	34.04	24.51	30.35	19.61
Res152	GAP [10]	34.04	34.67	52.85	61.61	58.09	59.24	50.08
	CDA [11]	29.33	34.88	44.28	46.05	46.91	51.62	42.17
	TAP [12]	33.25	37.53	41.18	42.14	50.96	56.45	43.58
	BIA [13]	22.82	27.44	34.66	36.74	45.48	51.26	36.40
	GAMA	16.43	17.02	21.93	17.07	31.63	30.57	22.44
	GAP [10]	42.79	45.01	57.79	65.42	63.02	65.31	56.55
Den169	CDA [11]	36.67	37.51	52.30	61.78	54.68	57.85	50.13
	TAP [12]	28.92	30.19	38.36	50.92	45.88	40.78	39.17
	BIA [13]	26.12	27.42	37.06	51.30	40.63	37.56	36.68
	GAMA	18.16	20.93	28.04	41.85	26.11	21.67	26.12

Table 5: MS-COCO \rightarrow ImageNet

$f(\cdot)$	Method	VGG16	VGG19	Res50	Res152	Den121	Den169	Average
VGG19	No Attack	70.15	70.94	74.60	77.34	74.22	75.74	73.83
	GAP [10]	15.55	15.06	49.50	56.07	47.65	53.49	39.55
	CDA [11]	13.05	12.59	46.77	52.58	43.55	50.03	36.42
	TAP [12]	02.33	02.93	19.28	35.20	19.45	23.42	17.10
	BIA [13]	02.51	03.09	29.72	43.98	30.37	36.53	24.36
	GAMA	02.01	02.57	19.99	35.21	26.26	32.98	19.83
Res152	GAP [10]	22.98	24.41	32.74	32.35	39.56	44.11	32.69
	CDA [11]	35.69	39.40	51.75	54.84	53.55	58.92	49.02
	TAP [12]	13.29	12.46	23.44	21.11	35.14	41.29	24.45
	BIA [13]	14.98	14.98	25.40	21.98	34.11	37.62	24.84
	GAMA	17.94	19.16	24.57	17.24	29.67	30.57	23.19
	GAP [10]	30.50	30.79	40.82	51.12	41.03	37.46	38.62
Den169	CDA [11]	35.75	36.69	50.45	57.43	51.23	52.44	47.33
	TAP [12]	21.45	26.45	27.30	45.76	30.83	25.34	29.52
	BIA [13]	20.91	25.01	37.16	50.65	34.71	23.38	31.97
	GAMA	06.94	10.63	10.97	21.60	13.92	08.22	12.04

Table 6: Pascal-VOC \rightarrow Coarse (CIFAR10/100) and Fine-grained (CUB, Car, Air) tasks

$f(\cdot)$	Method	CIFAR10	CIFAR100	CUB	CUB	CUB	Car	Car	Car	Air	Air	Air	Average
		[88]	[88]	Res50	SeNet	se-Res101	Res50	SeNet	se-Res101	Res50	SeNet	se-Res101	
VGG19	No Attack	93.79	74.28	87.35	86.81	86.54	94.35	93.36	92.97	92.23	92.05	91.90	89.60
	GAP [10]	73.58	39.10	78.94	79.79	80.41	82.33	85.71	87.19	81.19	81.82	79.99	77.27
	CDA [11]	70.40	44.68	54.76	64.74	68.99	70.87	75.64	81.78	42.87	74.38	77.20	66.02
	TAP [12]	73.18	35.41	72.42	74.39	73.94	78.40	77.08	84.59	78.91	78.94	75.52	72.98
	BIA [13]	59.82	27.84	68.31	65.64	73.70	75.61	67.90	81.83	75.88	66.13	76.75	67.22
	GAMA	53.85	24.94	53.52	62.19	66.93	60.08	69.11	78.95	45.51	43.71	63.37	56.56
Res152	GAP [10]	69.80	41.06	64.96	80.01	81.77	72.62	86.02	87.53	84.28	84.64	85.48	76.19
	CDA [11]	77.60	49.43	65.38	71.52	71.63	73.04	76.52	79.54	66.61	72.73	60.10	69.46
	TAP [12]	70.92	38.39	48.60	73.20	76.10	69.02	86.62	81.94	74.65	80.68	83.20	71.21
	BIA [13]	67.54	36.43	51.17	70.64	71.63	70.85	82.85	80.21	72.94	80.20	81.01	69.58
	GAMA	69.53	38.57	27.67	64.77	64.79	59.18	74.27	80.50	59.71	69.10	65.77	61.26
	GAP [10]	83.25	56.08	64.70	78.15	76.77	80.65	85.95	86.74	81.79	84.40	85.03	78.50
Den169	CDA [11]	84.34	58.03	61.75	73.40	71.75	84.21	85.57	84.58	78.97	82.24	78.22	76.64
	TAP [12]	86.77	58.67	54.04	64.45	62.31	76.13	81.35	82.91	34.02	76.66	76.75	68.55
	BIA [13]	85.20	55.21	47.95	58.18	56.02	55.88	73.65	72.30	62.47	72.97	70.39	64.56
	GAMA	78.27	46.80	33.57	57.44	63.24	49.31	70.65	75.14	48.48	62.95	70.15	59.63



(a) Custom architecture (both from [88])

(b) Standard architecture (left: Res50, right: se-Res101)

Figure 3: **Transferability on types of victim model designs.** GAMA shows potent transferring attacks to victim networks that were custom designed (Figure 3(a)) and that contain standard blocks like Residual blocks [80] (Figure 3(b)).

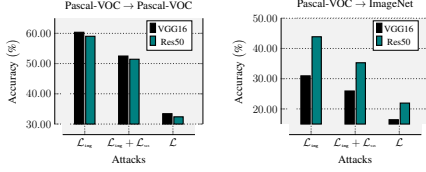


Figure 4: **Ablation analysis of loss objective.** We analyze the contribution due to the introduction of each loss function \mathcal{L}_{img} and \mathcal{L}_{ext} towards the final objective \mathcal{L} , both in same distribution (*left*) and different distribution (*right*). The surrogate model is Res152.

Table 7: Pascal-VOC \rightarrow MS-COCO Object Detection task

$f(\cdot)$	Method	FRCN	RNet	DETR	D ² ETR	Average
	No Attack	0.582	0.554	0.607	0.633	0.594
VGG19	GAP [10]	0.424	0.404	0.360	0.410	0.399
	CDA [11]	0.276	0.250	0.208	0.244	0.244
	TAP [12]	0.384	0.340	0.275	0.320	0.329
	BIA [13]	0.347	0.318	0.253	0.281	0.299
	GAMA	0.234	0.207	0.117	0.122	0.170
Res152	GAP [10]	0.389	0.362	0.363	0.408	0.380
	CDA [11]	0.305	0.274	0.256	0.281	0.279
	TAP [12]	0.400	0.348	0.288	0.350	0.346
	BIA [13]	0.321	0.275	0.205	0.256	0.264
	GAMA	0.172	0.138	0.080	0.095	0.121

Performance on Type of Architectures. In Figure 3, we further study the transferability of attacks depending on the type of victim architecture: *standard* which follow the standard modules like Residual blocks [80] to build the classifier, and *custom* where the victim classifier doesn’t adhere to a specific pattern of network modules. In both cases, **GAMA** consistently maintains better attack rates than other attacks. This shows convincing transferability of perturbations crafted from **GAMA**’s $\mathcal{G}_\theta(\cdot)$ under diverse black-box settings. We provide additional results in the supplementary material.

Robustness of Attacks against Defenses. To analyze the robustness of all the methods, we launch misclassification attacks ($\mathcal{G}_\theta(\cdot)$ trained on MS-COCO with the surrogate model as Den169) when the victim deploys input processing based defense such as median blur with window size as 3×3 , and Neural Representation purifier (NRP) [76] on three ImageNet models (VGG16, Res152, Den169). From Table 8(a) and Table 8(b), we can observe that the attack success of **GAMA** is better than prior methods even when the victim pre-processes the perturbed image before making decisions. In Figure 8(c), we observe that Projected Gradient Descent (PGD) [77] assisted Res50 is difficult to break with **GAMA** performing slightly better than other methods. Finally, motivated by [96], we analyze an output processing defense scenario where the victim can check the context consistency of predicted labels on perturbed images using the co-occurrence matrix \mathcal{O} . In particular, if a perturbed image is misclassified showing co-occurrence of labels not present in \mathcal{O} , we term this as a *detected attack*. Otherwise, we call it an *undetected attack*. To measure this performance, we first compute the co-occurrence matrix \mathcal{O}_δ by perturbing all the test set images and estimate its precision w.r.t. ground-truth \mathcal{O} . To check for attacks that have high precision value p and high misclassification rate, we calculate a ‘context score’ (higher is better) that is a harmonic mean of p and misclassification rate (1-accuracy). We show the attack performance against this context consistency check in Figure 8(d) for both Pascal-VOC and MS-COCO averaged over all surrogate models under white-box attacks. Clearly, **GAMA** presents itself as the best *undetected* attack compared to prior works.

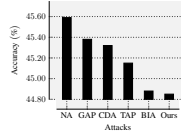
Ablation Analysis. We dissect the contribution of each loss function in our proposed loss objective of Equation (4) in Figure 4 where $\mathcal{G}_\theta(\cdot)$ is trained with Pascal-VOC with Res152 surrogate model. We analyze the attack transferability to different victim models (VGG16, Res50). We observe that the introduction of each loss objective (*left to right*) increases the strength of the attack both in the same distribution (Pascal-VOC) as the attacker and in the unknown distribution (ImageNet) on both victim classifiers. Finally, we visualize some perturbed image examples crafted by **GAMA** in Figure 5.

Method	VGG16	Res152	Den121	Average
No Attack	64.57	74.04	71.68	69.92
GAP [10]	33.33	56.90	46.34	45.52
CDA [11]	37.89	58.98	56.19	51.02
TAP [12]	22.37	50.67	40.81	37.95
BIA [13]	25.09	54.45	46.34	41.96
GAMA	20.34	49.66	37.55	35.85

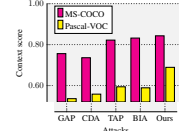
(a) Median Blur

Method	VGG16	Res152	Den121	Average
No Attack	56.26	62.37	68.62	62.41
GAP [10]	31.08	45.11	37.85	38.01
CDA [11]	34.61	47.64	51.32	44.52
TAP [12]	20.06	36.54	19.70	25.43
BIA [13]	19.94	41.03	20.07	23.68
GAMA	7.38	19.00	7.87	11.41

(b) NRP



(c) PGD ($\epsilon = 4$)



(d) Context check

Table 8: **Robustness Analysis against various defenses.** Our proposed attack **GAMA** consistently shows better performances compared to baselines in scenarios where the victim deploys attack defenses.

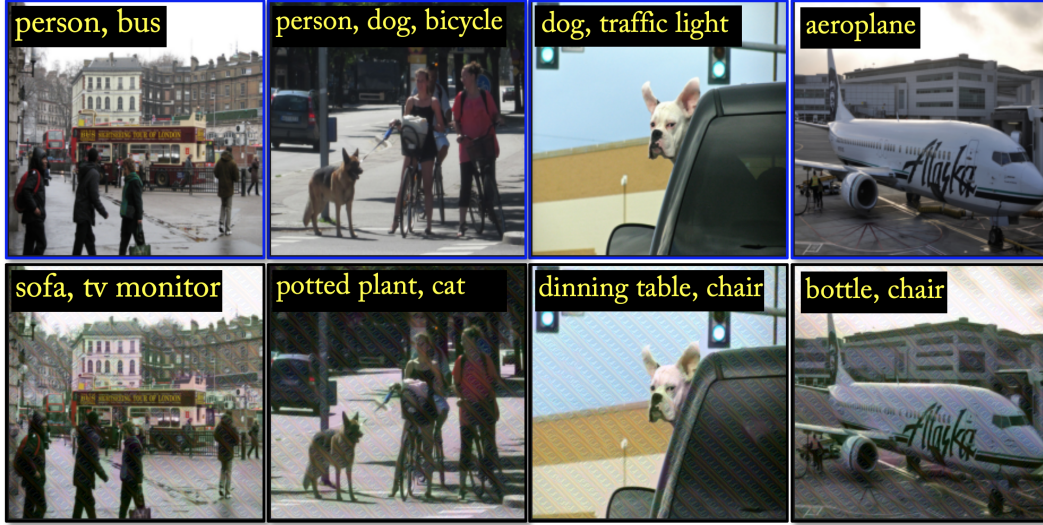


Figure 5: **Qualitative Examples.** We show some clean (*top*) and perturbed (*bottom*) images from **GAMA**. Best viewed in color/zoomed.

5 Conclusion

In this paper, we propose a new generative attack **GAMA** that can learn to create perturbations against multi-object scenes. For the first time in generative attack literature, we show the utility of a pre-trained vision-and-language model CLIP to optimize effectual perturbation generators. Specifically, CLIP’s joint text and image aligning property allow us to use natural language semantics in order to handle the multi-object semantics in the input scene to be perturbed. To demonstrate **GAMA**’s efficiency, we perform extensive experiments that show state-of-the-art attacks across a wide range of black-box victim models (multi-label/single-label classifiers, and object detectors). We also evaluate the robustness of our attacks against various defense mechanisms. As part of our future works, we will explore more complex methodologies to employ vision-language models both for adversarial attacks and defense systems.

6 Limitations and Societal Impacts

Limitations. The pre-trained CLIP model ‘ViT-B16’ outputs a 512-dimensional embedding that restricts us to compare the features extracted from the surrogate model in our losses of the same size. Another limitation of our method is the use of co-occurrence matrices to extract the right pair of classes that exist together in real-world scenes. In this paper, we make an assumption that text prompts are created using two classes that exist together according to the co-occurrence matrix of size $C \times C$ (for C classes in the data distribution). However, we can also use a triplet of classes that exist together in an input scene which would need a co-occurrence tensor of size $C \times C \times C$. Computing such a huge tensor would be tedious to cover all the images provided in the train set (usually in the order of thousands).

Societal Impacts. Adversarial attacks are designed with the sole goal to subvert machine decisions by any means available. Our attack approach shows one such method where a benign open-sourced vision-language model can be utilized by an attacker to create potent perturbations. This demonstrates the need for the victim to prepare for constantly evolving attacks that may cause major harm in real-world systems (*e.g.* person re-identification [97]). We believe that our work can help further propagate research into designing efficient and robust models that do not break down to attacks built upon multi-modal (in our case, text-image) features. Future researchers should also be aware of video generative models [98, 99] that can be used to create adversarial attacks for ubiquitous video classifiers built on the success of vision-language models.

Acknowledgement. This material is based upon work supported by the Defense Advanced Research Projects Agency (DARPA) under Agreement No. HR00112090096. Approved for public release; distribution is unlimited.

Supplementary material for “GAMA: Generative Adversarial Multi-Object Scene Attacks”

CONTENTS

A	Additional Analysis on GAMA	12
B	Additional Results w.r.t. Baselines	13
C	Implementation Details	15

List of Tables

1	Impact of CLIP model on GAMA	12
2	Random seed evaluations with error bars for GAMA	13
3	GAMA with surrogate ensemble (Pascal-VOC)	13
4	GAMA with surrogate ensemble (MS-COCO)	13
5	Black box attacks: MS-COCO object detection (MS-COCO \rightarrow MS-COCO)	13
6	Black-box attacks: Multi-label classification (Pascal-VOC \rightarrow MS-COCO)	13
7	Black-box attacks: Multi-label classification (MS-COCO \rightarrow Pascal-VOC)	13
8	Robustness analysis when $\mathcal{G}_\theta(\cdot)$ is trained on Pascal-VOC	14

List of Figures

1	Black-box Setting Embedding Visualization for GAMA and TAP [12]	12
2	Evaluation of adversarial images on CLIP	14

We present additional analysis of **GAMA** in the following sections to investigate its attack capabilities under various settings, including black-box embedding visualizations w.r.t. TAP [12], impact of different types of CLIP models, performance with ensemble of surrogate models. We also demonstrate **GAMA**’s transfer attack strength in comparison to prior methods under difficult black-box transfer attacks including in different multi-label distribution, object detection, and robustness of perturbations when victim uses defense mechanisms to minimize classifier performance deterioration. All experiments are done with perturbation budget $\ell_\infty \leq 10$.

A Additional Analysis on GAMA

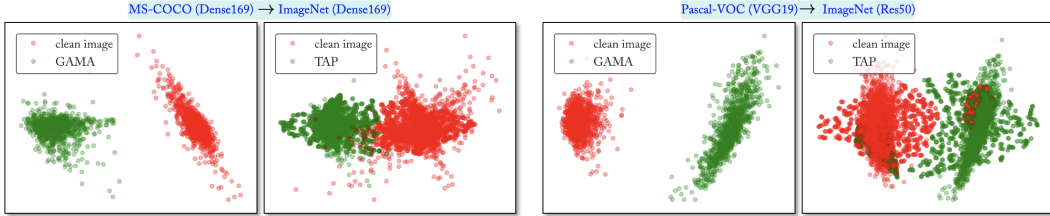


Figure 1: **Embedding visualization.** **GAMA** uses the CLIP extracted text and image embeddings to craft highly transferable adversarial examples. This can be seen in above embedding visualizations where **GAMA**’s perturbed images lie convincingly farther away from the clean images with better margins compared to TAP [12]. Left and right plots show perturbed image embeddings (both on random 1000 ImageNet images) when $\mathcal{G}_\theta(\cdot)$ is trained with MS-COCO and Pascal-VOC respectively. Surrogate and victim models are given in parenthesis.

Black-box Setting Embedding Visualization. To demonstrate the phenomenon that **GAMA** learns to create potent perturbations compared to prior works, we perform Principal Components Analysis (PCA) of perturbed images extracted from **GAMA** and TAP [12] in Figure 1 when the $\mathcal{G}_\theta(\cdot)$ is trained with MS-COCO and Pascal-VOC. We choose PCA visualization as it preserves the global differences of high dimensional data in low dimensional regimes [100, 101]. Clearly, in an unseen distribution (ImageNet [87]), features obtained from **GAMA**’s perturbed images significantly differ from those of clean images in comparison to TAP [12].

Impact of Different CLIP models. We analyze the impact of different open-source pre-trained CLIP models provided by Open-AI in Table 1 (surrogate model as Res152), both for the same domain and different domain transfer attacks. We observe that the CLIP frameworks with vision encoders with image transformers [102] (ViT-L/14, ViT-B/32, ViT-B/16) as their backbone perform better in our proposed setting than those with the vision encoders as convolutional networks (RN50, RN101). We attribute this to the effectual representation capability of transformers [102].

Table 1: Impact of CLIP model on **GAMA**

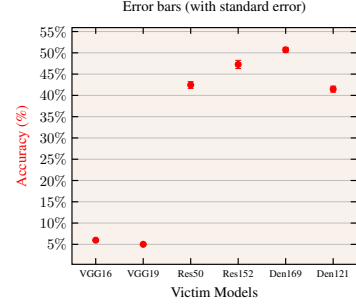
(a) Pascal-VOC → Pascal-VOC							(b) Pascal-VOC → ImageNet						
	VGG16	VGG19	Res50	Res152	Den169	Den121		VGG16	VGG19	Res50	Res152	Den121	Den169
No Attack	82.51	83.18	80.52	83.12	83.74	83.07	No Attack	70.15	70.94	74.60	77.34	74.22	75.74
RN50	8.83	15.25	64.37	67.24	70.53	69.13	RN50	3.13	2.06	46.25	52.01	49.33	45.91
RN101	21.74	9.45	60.56	68.53	67.01	66.17	RN101	2.93	2.41	42.73	56.16	46.67	45.97
ViT-L/14	43.35	49.89	45.08	43.30	54.23	51.53	ViT-L/14	16.63	20.04	26.41	23.18	31.10	32.53
ViT-B/32	10.58	15.18	67.07	70.34	69.14	68.02	ViT-B/32	3.90	2.81	49.61	54.41	48.02	46.41
ViT-B/16	6.12	5.89	41.17	45.57	53.11	44.58	ViT-B/16	3.07	3.41	22.32	34.04	24.51	30.35

Random Runs with Error Bars. We report the mean, and standard error in Table 2 along with the error bar plot (with mean and standard error). We can observe that **GAMA** maintains its performance with random seed values over various runs. Here, $\mathcal{G}_\theta(\cdot)$ was trained on Pascal-VOC with VGG19 as a surrogate.

Effect of Surrogate Ensemble. We analyze the results when all the surrogates (VGG19, Res152, and Den169) are employed together to train the perturbation generator $\mathcal{G}_\theta(\cdot)$ using **GAMA**. As can be seen in Table 3 and Table 4 (ensemble denoted as **All**), we do not observe any significant advantage in results when using multiple surrogates. This same observation has been noted by TAP

Table 2: Pascal-VOC \rightarrow Pascal-VOC (s.e. = standard error)

	VGG16	VGG19	Res50	Res152	Den169	Den121
No Attack	82.51	83.18	80.52	83.12	83.74	83.07
Run 1	5.86	5.18	45.43	50.88	52.61	43.44
Run 2	6.00	4.99	42.30	47.54	49.82	40.82
Run 3	6.08	4.88	40.71	46.64	50.31	42.73
Run 4	5.95	5.15	42.28	45.52	51.46	40.92
Run 5	6.01	4.84	41.47	45.77	49.33	39.47
mean	5.98	5.01	42.44	47.27	50.70	41.47
s.e.	0.035	0.067	0.800	0.966	0.590	0.711



[12] as well. We hypothesize that the mid-level features from multiple surrogates may not introduce complementary features to learn comparatively powerful perturbations than single classifier based surrogates.

Table 3: Ensemble comparison: VOC \rightarrow VOC

$f(\cdot)$	VGG16	VGG19	Res50	Res152	Den169	Den121	Average
VGG19	6.11	5.89	41.17	45.57	53.11	44.58	32.74
Res152	33.42	39.42	32.39	20.46	49.76	49.54	37.49
Den169	44.25	52.89	48.83	53.25	45.00	50.96	49.19
All	16.46	21.67	51.97	58.52	54.51	58.20	43.55

Table 4: Ensemble comparison: COCO \rightarrow COCO

$f(\cdot)$	VGG16	VGG19	Res50	Res152	Den169	Den121	Average
VGG19	3.59	3.75	27.13	30.43	24.60	21.77	18.54
Res152	24.52	27.73	30.62	23.04	31.30	27.31	27.42
Den169	10.40	13.47	19.30	23.46	8.65	10.29	14.26
All	10.08	10.75	23.83	35.23	29.57	30.45	23.32

Table 5: COCO \rightarrow COCO Object Detection

$f(\cdot)$	Method	FRCN	RNet	DETR	D ² ETR	Average
VGG19	No Attack	0.582	0.554	0.607	0.633	0.594
	GAP [10]	0.347	0.312	0.282	0.304	0.311
	CDA [11]	0.370	0.347	0.312	0.282	0.327
	TAP [12]	0.130	0.120	0.099	0.104	0.113
	BIA [13]	0.266	0.229	0.185	0.211	0.223
	GAMA	0.246	0.214	0.134	0.155	0.187
Res152	GAP [10]	0.187	0.145	0.097	0.108	0.134
	CDA [11]	0.322	0.301	0.237	0.274	0.283
	TAP [12]	0.167	0.151	0.087	0.123	0.132
	BIA [13]	0.152	0.144	0.101	0.121	0.129
	GAMA	0.154	0.128	0.086	0.100	0.117
	GAP [10]	0.308	0.261	0.201	0.213	0.245
Den169	CDA [11]	0.325	0.293	0.238	0.255	0.277
	TAP [12]	0.181	0.155	0.126	0.147	0.152
	BIA [13]	0.265	0.236	0.185	0.214	0.225
	GAMA	0.078	0.064	0.037	0.047	0.056

B Additional Results w.r.t. Baselines

Black-box Setting (Object Detection). We evaluate a black-box transfer attack with state-of-the-art MS-COCO object detectors (Faster RCNN with Res50 backbone (FRCN) [91], RetinaNet with Res50 backbone (RNet) [92], DETection TRansformer (DETR) [93], and Deformable DETR (D²ETR) [94]) in Table 5, provided by [95]. It can be observed that GAMA beats the baselines when $\mathcal{G}_\theta(\cdot)$ is trained with MS-COCO in the majority of scenarios.

Black-box Setting (Multi-Label Classification). We perform a black-box transfer attack on different multi-label domain than that of $\mathcal{G}_\theta(\cdot)$'s training set: Pascal-VOC \rightarrow MS-COCO in Table 6 and MS-COCO \rightarrow Pascal-VOC in Table 7. We outperform all baselines in the majority of cases, with an average absolute difference (w.r.t. closest method) of ~ 5 percentage points (pp) for Pascal-VOC \rightarrow MS-COCO, and ~ 13.5 pp for MS-COCO \rightarrow Pascal-VOC.

Table 6: Pascal-VOC \rightarrow MS-COCO

$f(\cdot)$	Method	VGG16	VGG19	Res50	Res152	Den169	Den121	Average
VGG19	No Attack	65.80	66.49	65.64	67.94	67.60	66.39	66.64
	GAP [10]	20.14	20.61	54.12	58.71	53.68	50.87	43.02
	CDA [11]	18.87	15.93	41.96	48.09	47.62	42.74	35.86
	TAP [12]	7.84	10.03	45.96	48.46	43.40	39.76	32.57
	BIA [13]	8.56	10.06	41.32	49.07	46.03	40.60	32.60
	GAMA	2.92	3.83	23.37	28.26	22.07	17.69	16.35
Res152	GAP [10]	32.90	33.63	46.70	54.18	53.71	51.40	45.41
	CDA [11]	27.28	32.25	41.32	44.59	48.33	45.10	39.81
	TAP [12]	31.68	37.33	36.09	36.85	47.77	45.59	39.22
	BIA [13]	26.99	29.83	33.86	35.35	45.87	41.70	35.59
	GAMA	21.43	28.59	29.54	24.95	32.92	29.89	27.89
	GAP [10]	42.64	44.07	50.14	57.48	57.01	53.16	50.75
Den169	CDA [11]	39.60	39.13	44.85	53.07	50.01	47.52	45.69
	TAP [12]	38.96	40.87	40.86	47.01	28.67	40.62	39.50
	BIA [13]	31.86	37.59	37.98	44.93	28.25	36.15	36.13
	GAMA	26.43	32.64	32.30	38.88	22.06	30.62	30.49

Table 7: MS-COCO \rightarrow Pascal-VOC

$f(\cdot)$	Method	VGG16	VGG19	Res50	Res152	Den169	Den121	Average
VGG19	No Attack	82.51	83.18	80.52	83.12	83.74	83.07	82.69
	GAP [10]	17.07	15.01	61.14	67.17	69.30	63.04	48.78
	CDA [11]	15.23	13.19	58.81	63.80	67.43	62.23	46.78
	TAP [12]	15.35	12.74	42.12	42.52	48.61	42.23	33.93
	BIA [13]	8.10	8.82	52.85	55.82	63.05	56.58	40.87
	GAMA	6.60	7.08	44.16	49.20	57.49	52.52	36.17
Res152	GAP [10]	27.09	28.45	45.91	37.28	58.07	51.28	41.34
	CDA [11]	53.45	55.82	64.68	64.12	70.74	65.04	62.31
	TAP [12]	42.21	41.26	41.02	35.35	58.99	54.77	45.60
	BIA [13]	37.04	36.46	44.91	36.12	54.60	49.95	43.18
	GAMA	36.86	40.62	38.23	23.52	48.56	48.03	39.30
	GAP [10]	48.37	46.35	58.04	60.73	52.89	57.83	54.03
Den169	CDA [11]	58.51	58.20	67.61	69.73	67.26	65.88	64.53
	TAP [12]	46.83	47.88	46.98	57.68	44.95	43.99	48.05
	BIA [13]	42.14	49.84	54.47	62.05	48.75	50.91	51.34
	GAMA	19.68	20.29	23.22	33.57	26.33	16.37	23.25

Robustness Analysis. We launch misclassification attacks ($\mathcal{G}_\theta(\cdot)$ trained on Pascal-VOC with the surrogate model as Den169) when the victim uses input processing based defense such as median blur with window size as 3×3 (Table 8(a)), and Neural Representation purifier (NRP) [76] (Table 8(b)) on three ImageNet models (VGG16, Res152, Den169). We can observe that the attack success of

GAMA is better than prior methods even when the victim pre-processes the perturbed image. Further, in Figure 8(c), we see that Projected Gradient Descent (PGD) [77] assisted Res50 is difficult to break with **GAMA** performing slightly better than other methods.

Method	VGG16	Res152	Den121	Average	Method	VGG16	Res152	Den121	Average
No Attack	64.57	74.04	71.68	69.92	No Attack	56.26	62.37	68.62	62.41
GAP [10]	47.91	65.64	61.69	58.41	GAP [10]	33.09	50.50	53.80	45.79
CDA [11]	33.62	58.70	50.12	47.48	CDA [11]	33.48	48.28	49.74	43.83
TAP [12]	23.92	48.89	43.66	38.82	TAP [12]	27.45	42.98	42.66	37.69
BIA [13]	24.49	50.96	40.29	38.58	BIA [13]	24.62	41.81	37.91	34.78
GAMA	22.84	52.10	36.19	37.04	GAMA	18.61	34.66	24.93	26.06

(a) Median Blur

(b) NRP

(c) PGD ($\epsilon = 8$)

Table 8: **Robustness Analysis against various defenses.** **GAMA** consistently shows better robustness in cases where victim uses attack defenses ($\mathcal{G}_\theta(\cdot)$ trained on Pascal-VOC). ‘NA’ in Figure 8(c) denotes ‘No Attack’.

Evaluation of adversarial images on CLIP. We evaluated CLIP (as a “zero-shot prediction” model) on the perturbed images from Pascal-VOC and computed the top two associated labels in Figure 2 using CLIP’s image-text aligning property. Specifically, we used the whole class list of Pascal-VOC and computed the top-2 associated labels both for clean and perturbed images. We can observe the perturbations change the labels associated with the clean image.

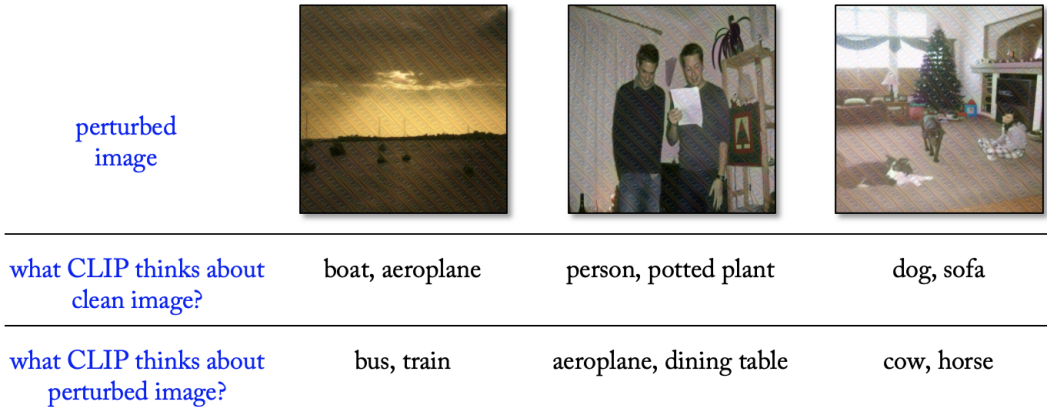


Figure 2: Evaluation of adversarial images on CLIP. Surrogate model is VGG19 trained on Pascal-VOC.

Mid-layer selection from surrogate model for training perturbation generator. Our mid-layer from surrogate model is chosen based on the embedding size of CLIP: *e.g.* if the embedding size of the CLIP encoder is 512, we select the layer from the surrogate model that outputs 512 dimension features. In comparison, prior state-of-the-art generative attack TAP [12] *manually* searches for the optimal layer from the surrogate model to train the perturbation generator (see *Limitations* in Section 4.6 in their paper [12]). In particular, finding the optimal mid-layer (that gives the best attack results) requires searching over each block of M layers (which is around an average of $M = 5$ layers [12]) for each surrogate model. Hence to find the best layer to train a perturbation generator for a particular model, the computation time cost for such an exhaustive search will be MN GPU hours where N is the total training time (in GPU hours) per layer. Moreover, our analysis shows this layer might not result in best attack results when the training data distribution varies and would require a manual search for all the different combinations of surrogate model and data distributions. Such a search is very time-consuming, impractical, and clearly not scalable. Finally, directly using TAP’s suggested layer is not possible because the embedding size doesn’t match that of CLIP, and would require us to introduce embedding modifications mechanisms (*e.g.* Principal Component Analysis (PCA), t-distributed stochastic neighbor embedding (t-SNE)) leading to an unreasonable increase in training time for every epoch. Note that if we do not consider the manual search of an optimal layer from the surrogate model to train the perturbation generator, then the proper baseline on ImageNet would be CDA [11]. As evident throughout our analysis, we convincingly outperform them on all settings.

C Implementation Details

We use two multi-label datasets to stimulate the scenario of multi-object scenes: Pascal-VOC (training set: *trainval* from ‘VOC2007’ and ‘VOC2012’, testing set: ‘VOC2007_test’) and MS-COCO (training set: *train2017*, testing set: *val2017*). We follow prior works [11, 13] for the generator network for $\mathcal{G}_\theta(\cdot)$. To stabilize the training, we replace all the ReLU [103] activation functions with Fused Leaky ReLU [104] activation function (negative slope = 0.2, scale = $\sqrt{2}$). We use a margin $\alpha = 1.0$ for the contrastive loss. All our training setup uses ViT-B/16 as the CLIP model. We use Adam optimizer [75] with a learning rate 0.0001, batch size 16, and exponential decay rates between 0.5 and 0.999. All images were resized to 224×224 . Training time was observed to be ~ 1 hr for Pascal-VOC dataset (10 epochs) and ~ 10 hrs for MS-COCO dataset (5 epochs) on one NVIDIA GeForce RTX 3090 GPUs. PyTorch is employed [105] in all code implementations.

References

- [1] Christian Szegedy, Wojciech Zaremba, Ilya Sutskever, Joan Bruna, Dumitru Erhan, Ian Goodfellow, and Rob Fergus. Intriguing Properties of Neural Networks. *arXiv preprint arXiv:1312.6199*, 2013.
- [2] Ian J Goodfellow, Jonathon Shlens, and Christian Szegedy. Explaining and Harnessing Adversarial Examples. *arXiv preprint arXiv:1412.6572*, 2014.
- [3] Linxi Jiang, Xingjun Ma, Shaoxiang Chen, James Bailey, and Yu-Gang Jiang. Black-box adversarial attacks on video recognition models. In *Proceedings of the 27th ACM International Conference on Multimedia*, pages 864–872, 2019.
- [4] Huanqian Yan, Xingxing Wei, and Bo Li. Sparse black-box video attack with reinforcement learning. *arXiv preprint arXiv:2001.03754*, 2020.
- [5] Zhipeng Wei, Jingjing Chen, Xingxing Wei, Linxi Jiang, Tat-Seng Chua, Fengfeng Zhou, and Yu-Gang Jiang. Heuristic black-box adversarial attacks on video recognition models. In *Proceedings of the AAAI Conference on Artificial Intelligence*, pages 12338–12345, 2020.
- [6] Shasha Li, Abhishek Aich, Shitong Zhu, Salman Asif, Chengyu Song, Amit Roy-Chowdhury, and Srikanth Krishnamurthy. Adversarial attacks on black box video classifiers: Leveraging the power of geometric transformations. *Advances in Neural Information Processing Systems*, 34, 2021.
- [7] Hu Zhang, Linchao Zhu, Yi Zhu, and Yi Yang. Motion-excited sampler: Video adversarial attack with sparked prior. In *European Conference on Computer Vision*. Springer, 2020.
- [8] Nicholas Carlini and David Wagner. Towards evaluating the robustness of neural networks. In *2017 IEEE symposium on security and privacy (sp)*, pages 39–57. IEEE, 2017.
- [9] Seyed-Mohsen Moosavi-Dezfooli, Alhussein Fawzi, and Pascal Frossard. Deepfool: A Simple and Accurate Method to Fool Deep Neural Networks. In *Proceedings of the IEEE conference on computer vision and pattern recognition*, pages 2574–2582. IEEE, 2016.
- [10] Omid Poursaeed, Isay Katsman, Bicheng Gao, and Serge Belongie. Generative Adversarial Perturbations. In *Proceedings of the IEEE Conference on Computer Vision and Pattern Recognition*, pages 4422–4431. IEEE, 2018.
- [11] Muzammal Naseer, Salman H Khan, Harris Khan, Fahad Shahbaz Khan, and Fatih Porikli. Cross-Domain Transferability of Adversarial Perturbations. *arXiv preprint arXiv:1905.11736*, 2019.
- [12] Mathieu Salzmann et al. Learning transferable adversarial perturbations. *Advances in Neural Information Processing Systems*, 34, 2021.
- [13] Qilong Zhang, Xiaodan Li, YueFeng Chen, Jingkuan Song, Lianli Gao, Yuan He, and Hui Xue’. Beyond imagenet attack: Towards crafting adversarial examples for black-box domains. In *International Conference on Learning Representations*. International Conference on Learning Representations (ICLR), 2022.

- [14] Alexey Kurakin, Ian Goodfellow, and Samy Bengio. Adversarial machine learning at scale. *arXiv preprint arXiv:1611.01236*, 2016.
- [15] Anh Nguyen, Jason Yosinski, and Jeff Clune. Deep Neural Networks are Easily Fooled: High Confidence Predictions for Unrecognizable Images. In *Proceedings of the IEEE conference on computer vision and pattern recognition*, pages 427–436. IEEE, 2015.
- [16] Qingquan Song, Haifeng Jin, Xiao Huang, and Xia Hu. Multi-label adversarial perturbations. In *2018 IEEE International Conference on Data Mining (ICDM)*, pages 1242–1247. IEEE, 2018.
- [17] Nan Zhou, Wenjian Luo, Xin Lin, Peilan Xu, and Zhenya Zhang. Generating multi-label adversarial examples by linear programming. In *2020 International Joint Conference on Neural Networks (IJCNN)*, pages 1–8. IEEE, 2020.
- [18] Shaohao Lu, Yuqiao Xian, Ke Yan, Yi Hu, Xing Sun, Xiaowei Guo, Feiyue Huang, and Wei-Shi Zheng. Discriminator-free generative adversarial attack. In *Proceedings of the 29th ACM International Conference on Multimedia*, pages 1544–1552. ACM, 2021.
- [19] Alex Krizhevsky, Ilya Sutskever, and Geoffrey E Hinton. Imagenet classification with deep convolutional neural networks. *Advances in neural information processing systems*, 25, 2012.
- [20] Matthew R Boutell, Jiebo Luo, Xipeng Shen, and Christopher M Brown. Learning multi-label scene classification. *Pattern recognition*, 37(9):1757–1771, 2004.
- [21] Min-Ling Zhang and Zhi-Hua Zhou. Ml-knn: A lazy learning approach to multi-label learning. *Pattern recognition*, 40(7):2038–2048, 2007.
- [22] Jesse Read, Bernhard Pfahringer, Geoff Holmes, and Eibe Frank. Classifier chains for multi-label classification. *Machine learning*, page 333, 2011.
- [23] Shang-Fu Chen, Yi-Chen Chen, Chih-Kuan Yeh, and Yu-Chiang Wang. Order-free rnn with visual attention for multi-label classification. In *Proceedings of the AAAI Conference on Artificial Intelligence*. AAAI, 2018.
- [24] Erin L Allwein, Robert E Schapire, and Yoram Singer. Reducing multiclass to binary: A unifying approach for margin classifiers. *Journal of machine learning research*, 1(Dec): 113–141, 2000.
- [25] Zhao-Min Chen, Xiu-Shen Wei, Peng Wang, and Yanwen Guo. Multi-Label Image Recognition with Graph Convolutional Networks. In *The IEEE Conference on Computer Vision and Pattern Recognition (CVPR)*. IEEE, 2019.
- [26] Zikui Cai, Shantanu Rane, Alejandro E Brito, Chengyu Song, Srikanth V Krishnamurthy, Amit K Roy-Chowdhury, and M Salman Asif. Zero-query transfer attacks on context-aware object detectors. *arXiv preprint arXiv:2203.15230*, 2022.
- [27] Zikui Cai, Xinxin Xie, Shasha Li, Mingjun Yin, Chengyu Song, Srikanth V Krishnamurthy, Amit K Roy-Chowdhury, and M Salman Asif. Context-aware transfer attacks for object detection. *arXiv preprint arXiv:2112.03223*, 2021.
- [28] Chawin Sitawarin, Arjun Nitin Bhagoji, Arsalan Mosenia, Mung Chiang, and Prateek Mittal. Darts: Deceiving autonomous cars with toxic signs. *arXiv preprint arXiv:1802.06430*, 2018.
- [29] Shang-Tse Chen, Cory Cornelius, Jason Martin, and Duen Horng Polo Chau. Shapeshifter: Robust physical adversarial attack on faster r-cnn object detector. In *Joint European Conference on Machine Learning and Knowledge Discovery in Databases*, pages 52–68. Springer, 2018.
- [30] Mingjun Yin, Shasha Li, Zikui Cai, Chengyu Song, M Salman Asif, Amit K Roy-Chowdhury, and Srikanth V Krishnamurthy. Exploiting multi-object relationships for detecting adversarial attacks in complex scenes. In *Proceedings of the IEEE/CVF International Conference on Computer Vision*, pages 7858–7867, 2021.
- [31] Chaowei Xiao, Bo Li, Jun-Yan Zhu, Warren He, Mingyan Liu, and Dawn Song. Generating Adversarial Examples with Adversarial Networks. *arXiv preprint arXiv:1801.02610*, 2018.

- [32] Catherine Wah, Steve Branson, Peter Welinder, Pietro Perona, and Serge Belongie. The caltech-ucsd birds-200-2011 dataset. 2011.
- [33] PyTorch. Imagenet models and pre-trained weights. PyTorch, 2022. URL <https://pytorch.org/vision/stable/models.html>.
- [34] Claudine Badue, Rânik Guidolini, Raphael Vivacqua Carneiro, Pedro Azevedo, Vinicius B Cardoso, Avelino Forechi, Luan Jesus, Rodrigo Berriel, Thiago M Paixao, Filipe Mutz, et al. Self-driving cars: A survey. *Expert Systems with Applications*, 165:113816, 2021.
- [35] Chao Jia, Yinfei Yang, Ye Xia, Yi-Ting Chen, Zarana Parekh, Hieu Pham, Quoc Le, Yun-Hsuan Sung, Zhen Li, and Tom Duerig. Scaling up visual and vision-language representation learning with noisy text supervision. In *International Conference on Machine Learning*, pages 4904–4916. PMLR, 2021.
- [36] Alec Radford, Jong Wook Kim, Chris Hallacy, Aditya Ramesh, Gabriel Goh, Sandhini Agarwal, Girish Sastry, Amanda Askell, Pamela Mishkin, Jack Clark, et al. Learning transferable visual models from natural language supervision. In *International Conference on Machine Learning*, pages 8748–8763. PMLR, 2021.
- [37] Norman Mu, Alexander Kirillov, David Wagner, and Saining Xie. Slip: Self-supervision meets language-image pre-training. *arXiv preprint arXiv:2112.12750*, 2021.
- [38] Yangguang Li, Feng Liang, Lichen Zhao, Yufeng Cui, Wanli Ouyang, Jing Shao, Fengwei Yu, and Junjie Yan. Supervision exists everywhere: A data efficient contrastive language-image pre-training paradigm. *arXiv preprint arXiv:2110.05208*, 2021.
- [39] Lewei Yao, Runhui Huang, Lu Hou, Guansong Lu, Minzhe Niu, Hang Xu, Xiaodan Liang, Zhenguo Li, Xin Jiang, and Chunjing Xu. Filip: Fine-grained interactive language-image pre-training. *arXiv preprint arXiv:2111.07783*, 2021.
- [40] Huaishao Luo, Lei Ji, Ming Zhong, Yang Chen, Wen Lei, Nan Duan, and Tianrui Li. Clip4clip: An empirical study of clip for end to end video clip retrieval. *arXiv preprint arXiv:2104.08860*, 2021.
- [41] Or Patashnik, Zongze Wu, Eli Shechtman, Daniel Cohen-Or, and Dani Lischinski. Styleclip: Text-driven manipulation of stylegan imagery. In *Proceedings of the IEEE/CVF International Conference on Computer Vision*, pages 2085–2094, 2021.
- [42] Apoorv Khandelwal, Luca Weihs, Roozbeh Mottaghi, and Aniruddha Kembhavi. Simple but effective: Clip embeddings for embodied ai. *arXiv preprint arXiv:2111.09888*, 2021.
- [43] Aditya Ramesh, Prafulla Dhariwal, Alex Nichol, Casey Chu, and Mark Chen. Hierarchical text-conditional image generation with clip latents. *arXiv preprint arXiv:2204.06125*, 2022.
- [44] Aditya Ramesh, Mikhail Pavlov, Gabriel Goh, Scott Gray, Chelsea Voss, Alec Radford, Mark Chen, and Ilya Sutskever. Zero-shot text-to-image generation. In *International Conference on Machine Learning*, pages 8821–8831. PMLR, 2021.
- [45] Marcos V Conde and Kerem Turgutlu. Clip-art: contrastive pre-training for fine-grained art classification. In *Proceedings of the IEEE/CVF Conference on Computer Vision and Pattern Recognition*, pages 3956–3960, 2021.
- [46] Rinon Gal, Or Patashnik, Haggai Maron, Gal Chechik, and Daniel Cohen-Or. Stylegan-nada: Clip-guided domain adaptation of image generators. *arXiv preprint arXiv:2108.00946*, 2021.
- [47] Aditya Sanghi, Hang Chu, Joseph G Lambourne, Ye Wang, Chin-Yi Cheng, and Marco Fumero. Clip-forged: Towards zero-shot text-to-shape generation. *arXiv preprint arXiv:2110.02624*, 2021.
- [48] Gwanghyun Kim and Jong Chul Ye. Diffusionclip: Text-guided image manipulation using diffusion models. *arXiv preprint arXiv:2110.02711*, 2021.
- [49] Gihyun Kwon and Jong Chul Ye. Clipstyler: Image style transfer with a single text condition. *arXiv preprint arXiv:2112.00374*, 2021.

- [50] Yongming Rao, Wenliang Zhao, Guangyi Chen, Yansong Tang, Zheng Zhu, Guan Huang, Jie Zhou, and Jiwen Lu. Denseclip: Language-guided dense prediction with context-aware prompting. In *Proceedings of the IEEE Conference on Computer Vision and Pattern Recognition (CVPR)*, 2022.
- [51] Manling Li, Ruochen Xu, Shuohang Wang, Luowei Zhou, Xudong Lin, Chenguang Zhu, Michael Zeng, Heng Ji, and Shih-Fu Chang. Clip-event: Connecting text and images with event structures. *arXiv preprint arXiv:2201.05078*, 2022.
- [52] Alhussein Fawzi, Omar Fawzi, and Pascal Frossard. Analysis of Classifiers’ Robustness to Adversarial Perturbations. *Machine Learning*, pages 481–508, 2018.
- [53] Aishan Liu, Xianglong Liu, Jiaxin Fan, Yuqing Ma, Anlan Zhang, Huiyuan Xie, and Dacheng Tao. Perceptual-Sensitive GAN for Generating Adversarial Patches. In *Proceedings of the AAAI conference on artificial intelligence*, pages 1028–1035. AAAI, 2019.
- [54] Jiangfan Han, Xiaoyi Dong, Ruimao Zhang, Dongdong Chen, Weiming Zhang, Nenghai Yu, Ping Luo, and Xiaogang Wang. Once a MAN: Towards Multi-Target Attack via Learning Multi-Target Adversarial Network Once. In *Proceedings of the IEEE/CVF International Conference on Computer Vision*, pages 5158–5167. IEEE, 2019.
- [55] Chaowei Xiao, Jun-Yan Zhu, Bo Li, Warren He, Mingyan Liu, and Dawn Song. Spatially transformed adversarial examples. *arXiv preprint arXiv:1801.02612*, 2018.
- [56] Krishna Kanth Nakka and Mathieu Salzmann. Indirect local attacks for context-aware semantic segmentation networks. In *European Conference on Computer Vision*, pages 611–628. Springer, 2020.
- [57] Shu Hu, Lipeng Ke, Xin Wang, and Siwei Lyu. Tkml-ap: Adversarial attacks to top-k multi-label learning. In *Proceedings of the IEEE/CVF International Conference on Computer Vision*, pages 7649–7657. IEEE, 2021.
- [58] Yinpeng Dong, Fangzhou Liao, Tianyu Pang, Hang Su, Jun Zhu, Xiaolin Hu, and Jianguo Li. Boosting Adversarial Attacks with Momentum. In *Proceedings of the IEEE conference on computer vision and pattern recognition*, pages 9185–9193. IEEE, 2018.
- [59] Yanbo Fan, Baoyuan Wu, Tuanhui Li, Yong Zhang, Mingyang Li, Zhifeng Li, and Yujiu Yang. Sparse adversarial attack via perturbation factorization. In *Computer Vision–ECCV 2020: 16th European Conference, Glasgow, UK, August 23–28, 2020, Proceedings, Part XXII 16*, pages 35–50. Springer, 2020.
- [60] Anand Bhattad, Min Jin Chong, Kaizhao Liang, Bo Li, and David A Forsyth. Unrestricted adversarial examples via semantic manipulation. *arXiv preprint arXiv:1904.06347*, 2019.
- [61] Haonan Qiu, Chaowei Xiao, Lei Yang, Xinchun Yan, Honglak Lee, and Bo Li. Semanti-cadv: Generating adversarial examples via attribute-conditioned image editing. In *European Conference on Computer Vision*, pages 19–37. Springer, 2020.
- [62] Alexia Jolicoeur-Martineau. The relativistic discriminator: a key element missing from standard gan. In *International Conference on Learning Representations*, 2018.
- [63] Han Fang, Pengfei Xiong, Luhui Xu, and Yu Chen. Clip2video: Mastering video-text retrieval via image clip. *arXiv preprint arXiv:2106.11097*, 2021.
- [64] Karen Simonyan and Andrew Zisserman. Very Deep Convolutional Networks for Large-Scale Image Recognition. *arXiv preprint arXiv:1409.1556*, 2014.
- [65] Justin Johnson, Alexandre Alahi, and Li Fei-Fei. Perceptual Losses for Real-Time Style Transfer and Super-Resolution. In *European conference on computer vision*, pages 694–711. Springer, 2016.
- [66] Roey Mechrez, Itamar Talmi, and Lihi Zelnik-Manor. The contextual loss for image transformation with non-aligned data. In *Proceedings of the European conference on computer vision (ECCV)*, pages 768–783, 2018.

- [67] Jack Hessel, Ari Holtzman, Maxwell Forbes, Ronan Le Bras, and Yejin Choi. CLIPScore: a reference-free evaluation metric for image captioning. In *EMNLP*, 2021.
- [68] Kaiyang Zhou, Jingkang Yang, Chen Change Loy, and Ziwei Liu. Conditional prompt learning for vision-language models. In *CVPR*, 2022.
- [69] Zhao-Min Chen, Xiu-Shen Wei, Peng Wang, and Yanwen Guo. Multi-label image recognition with graph convolutional networks. In *Proceedings of the IEEE/CVF conference on computer vision and pattern recognition*, pages 5177–5186, 2019.
- [70] Md Amirul Islam, Matthew Kowal, Konstantinos G Derpanis, and Neil DB Bruce. Segmix: Co-occurrence driven mixup for semantic segmentation and adversarial robustness. *arXiv preprint arXiv:2108.09929*, 2021.
- [71] Hang Zhang, Han Zhang, Chenguang Wang, and Junyuan Xie. Co-occurrent features in semantic segmentation. In *Proceedings of the IEEE/CVF Conference on Computer Vision and Pattern Recognition*, pages 548–557, 2019.
- [72] Md Amirul Islam, Matthew Kowal, Konstantinos G Derpanis, and Neil DB Bruce. Feature binding with category-dependant mixup for semantic segmentation and adversarial robustness. *arXiv preprint arXiv:2008.05667*, 2020.
- [73] Raia Hadsell, Sumit Chopra, and Yann LeCun. Dimensionality reduction by learning an invariant mapping. In *2006 IEEE Computer Society Conference on Computer Vision and Pattern Recognition (CVPR'06)*, volume 2, pages 1735–1742. IEEE, 2006.
- [74] Ching-Yao Chuang, Joshua Robinson, Yen-Chen Lin, Antonio Torralba, and Stefanie Jegelka. Debaised contrastive learning. *Advances in neural information processing systems*, 33:8765–8775, 2020.
- [75] Diederik P Kingma and Jimmy Ba. Adam: A Method for Stochastic Optimization. *arXiv preprint arXiv:1412.6980*, 2014.
- [76] Muzammal Naseer, Salman Khan, Munawar Hayat, Fahad Shahbaz Khan, and Fatih Porikli. A self-supervised approach for adversarial robustness. In *Proceedings of the IEEE/CVF Conference on Computer Vision and Pattern Recognition*, pages 262–271, 2020.
- [77] Aleksander Madry, Aleksandar Makelov, Ludwig Schmidt, Dimitris Tsipras, and Adrian Vladu. Towards deep learning models resistant to adversarial attacks. *arXiv preprint arXiv:1706.06083*, 2017.
- [78] Mark Everingham, Luc Van Gool, Christopher KI Williams, John Winn, and Andrew Zisserman. The Pascal Visual Object Classes (VOC) Challenge. *International journal of computer vision*, 88(2):303–338, 2010.
- [79] Tsung-Yi Lin, Michael Maire, Serge Belongie, James Hays, Pietro Perona, Deva Ramanan, Piotr Dollár, and C Lawrence Zitnick. Microsoft COCO: Common Objects in Context. In *European conference on computer vision*, pages 740–755. Springer, 2014.
- [80] Kaiming He, Xiangyu Zhang, Shaoqing Ren, and Jian Sun. Deep Residual Learning for Image Recognition. In *Proceedings of the IEEE conference on computer vision and pattern recognition*, pages 770–778. IEEE, 2016.
- [81] Gao Huang, Zhuang Liu, Laurens Van Der Maaten, and Kilian Q Weinberger. Densely Connected Convolutional Networks. In *Proceedings of the IEEE conference on computer vision and pattern recognition*, pages 4700–4708. IEEE, 2017.
- [82] Shantanu Godbole and Sunita Sarawagi. Discriminative methods for multi-labeled classification. In *Pacific-Asia conference on knowledge discovery and data mining*, pages 22–30. Springer, 2004.
- [83] Mohammad S Sorower. A literature survey on algorithms for multi-label learning. *Oregon State University, Corvallis*, 18:1–25, 2010.

- [84] Alex Krizhevsky, Geoffrey Hinton, et al. Learning multiple layers of features from tiny images. 2009.
- [85] Jonathan Krause, Jia Deng, Michael Stark, and Li Fei-Fei. Collecting a large-scale dataset of fine-grained cars. 2013.
- [86] Subhransu Maji, Esa Rahtu, Juho Kannala, Matthew Blaschko, and Andrea Vedaldi. Fine-grained visual classification of aircraft. *arXiv preprint arXiv:1306.5151*, 2013.
- [87] Jia Deng, Wei Dong, Richard Socher, Li-Jia Li, Kai Li, and Li Fei-Fei. Imagenet: A large-scale hierarchical image database. In *2009 IEEE conference on computer vision and pattern recognition*, pages 248–255. IEEE, 2009.
- [88] Aaron Chen. Coarse-grain models and pre-trained weights. GitHub link, 2022. URL <https://github.com/aaron-xichen/pytorch-playground>.
- [89] Jie Hu, Li Shen, and Gang Sun. Squeeze-and-excitation networks. In *Proceedings of the IEEE conference on computer vision and pattern recognition*, pages 7132–7141. IEEE, 2018.
- [90] Alibaba-AAIG. Fine-grain models and pre-trained weights. GitHub link, 2022. URL https://github.com/Alibaba-AAIG/Beyond-ImageNet-Attack/releases/download/Pretrained_DCL_model/model.zip.
- [91] Ross Girshick. Fast r-cnn. In *Proceedings of the IEEE international conference on computer vision*, 2015.
- [92] Tsung-Yi Lin, Priya Goyal, Ross Girshick, Kaiming He, and Piotr Dollár. Focal loss for dense object detection. In *Proceedings of the IEEE international conference on computer vision*, 2017.
- [93] Nicolas Carion, Francisco Massa, Gabriel Synnaeve, Nicolas Usunier, Alexander Kirillov, and Sergey Zagoruyko. End-to-end object detection with transformers. In *ECCV*, 2020.
- [94] Xizhou Zhu, Weijie Su, Lewei Lu, Bin Li, Xiaogang Wang, and Jifeng Dai. Deformable detr: Deformable transformers for end-to-end object detection. In *International Conference on Learning Representations*, 2021. URL <https://openreview.net/forum?id=gZ9hCDWe6ke>.
- [95] Kai Chen, Jiaqi Wang, Jiangmiao Pang, Yuhang Cao, Yu Xiong, Xiaoxiao Li, Shuyang Sun, Wansen Feng, Ziwei Liu, Jiarui Xu, Zheng Zhang, Dazhi Cheng, Chenchen Zhu, Tianheng Cheng, Qijie Zhao, Buyu Li, Xin Lu, Rui Zhu, Yue Wu, Jifeng Dai, Jingdong Wang, Jianping Shi, Wanli Ouyang, Chen Change Loy, and Dahua Lin. MMDetection: Open mmlab detection toolbox and benchmark. *arXiv preprint arXiv:1906.07155*, 2019.
- [96] Shasha Li, Shitong Zhu, Sudipta Paul, Amit Roy-Chowdhury, Chengyu Song, Srikanth Krishnamurthy, Ananthram Swami, and Kevin S Chan. Connecting the Dots: Detecting Adversarial Perturbations Using Context Inconsistency. In *European Conference on Computer Vision*, pages 396–413. Springer, 2020.
- [97] Abhishek Aich, Meng Zheng, Srikrishna Karanam, Terrence Chen, Amit K. Roy-Chowdhury, and Ziyang Wu. Spatio-temporal representation factorization for video-based person re-identification. In *Proceedings of the IEEE/CVF International Conference on Computer Vision (ICCV)*, pages 152–162, October 2021.
- [98] Abhishek Aich, Akash Gupta, Rameswar Panda, Rakib Hyder, M. Salman Asif, and Amit K. Roy-Chowdhury. Non-adversarial video synthesis with learned priors. In *Proceedings of the IEEE/CVF Conference on Computer Vision and Pattern Recognition (CVPR)*, June 2020.
- [99] Akash Gupta, Abhishek Aich, and Amit K Roy-Chowdhury. Alanet: Adaptive latent attention network for joint video deblurring and interpolation. In *Proceedings of the 28th ACM International Conference on Multimedia*, pages 256–264, 2020.
- [100] Abubakar Abid, Martin J Zhang, Vivek K Bagaria, and James Zou. Exploring patterns enriched in a dataset with contrastive principal component analysis. *Nature communications*, 9(1):1–7, 2018.

- [101] Takanori Fujiwara, Oh-Hyun Kwon, and Kwan-Liu Ma. Supporting analysis of dimensionality reduction results with contrastive learning. *IEEE transactions on visualization and computer graphics*, 26(1):45–55, 2019.
- [102] Alexey Dosovitskiy, Lucas Beyer, Alexander Kolesnikov, Dirk Weissenborn, Xiaohua Zhai, Thomas Unterthiner, Mostafa Dehghani, Matthias Minderer, Georg Heigold, Sylvain Gelly, et al. An image is worth 16x16 words: Transformers for image recognition at scale. *arXiv preprint arXiv:2010.11929*, 2020.
- [103] Vinod Nair and Geoffrey E Hinton. Rectified linear units improve restricted boltzmann machines. In *ICML*. ICML, 2010.
- [104] Tero Karras, Samuli Laine, and Timo Aila. A style-based generator architecture for generative adversarial networks. In *Proceedings of the IEEE/CVF conference on computer vision and pattern recognition*, pages 4401–4410. IEEE, 2019.
- [105] Adam Paszke, Sam Gross, Francisco Massa, Adam Lerer, James Bradbury, Gregory Chanan, Trevor Killeen, Zeming Lin, Natalia Gimelshein, Luca Antiga, et al. PyTorch: An Imperative Style, High-Performance Deep Learning Library. In *Advances in Neural Information Processing Systems*, pages 8026–8037. NeurIPS, 2019.